Computing and Visualization in Science manuscript No.
(will be inserted by the editor)

Flux-based methods of characteristics for coupled transport equations in porous media

Peter Frolkovič *

Simulation in Technology Center, IWR, Im Neuenheimer Feld 368, D-69120 Heidelberg, Germany
(http://www.iwr.uni-heidelberg.de/~Peter.Frolkovic)

The date of receipt and acceptance will be inserted by the editor

Abstract. Mathematical models of transport of radioactive contaminants in flowing groundwater involve large systems of coupled advection dominated transport equations. High-resolution explicit finite volume methods, if applied to advective part of model and combined with appropriate numerical methods for diffusion-dispersion-reaction part, can offer precise and monotone numerical solutions, but they require small time steps. This paper describes Flux-Based Methods Of Characteristics that are extension of explicit finite volume methods, that have no restriction on time steps and that produce numerical solutions with valid discrete minimum and maximum principle. Such particular method was implemented in software package R^3T (Retardation, Reaction, Radionuclides and Transport) and it was used successfully to solve large systems of coupled transport equations with different retardation factors for transport.

1 Introduction

Mathematical models of transport in groundwater flow that are used in risk scenarios for radioactive waste disposals, require extremely long time simulations, see e.g. [2]. Consequently, this type of problems demands numerical methods that allow large time steps with no excessive loss of precision and with no unphysical behaviour of numerical solutions.

Typically, transport equations for this type of problems are coupled through chemical reactions and different chemical properties of each radionuclide can cause different retardation of transport. In such a way, the resulting mathematical models [10] are difficult to solve by standard numerical methods.

It is well-known that high-resolution explicit Finite Volume Methods (FVM) are suitable for the approximation of advective transport [18]. If these methods are used through operator splitting approach with appropriate numerical algorithms for diffusion-dispersion-reaction part of problem, precise numerical solutions for general transport models can be obtained. Moreover, such methods preserve local and global mass balance property, they can treat properly general boundary conditions, and they reduce unphysical smearing of solutions by numerical dispersion.

Nevertheless, the explicit FVM are designed to be used only with "enough small" time steps (the so called "CFL condition").

This problem of "Eulerian type of methods" (that are based on fixed coordinates in time) can be removed by applying "Lagrangian type of methods". Such methods use moving coordinates to track characteristic curves determined by groundwater velocities. Too many numerical methods to be listed here were developed in this framework. We mention only Finite Volume Eulerian-Lagrangian Localized Adjoint Methods (FV-ELLAM) [13] that are the most successful in conserving the properties of finite volume methods and in removing the restriction on the choice of time steps, see also [25]. Nevertheless, the published FV-ELLAM implementations [3,14] can not be viewed as a direct extension of finite volume ("flux-based") discretization schemes. Only recently, a flux-based form of ELLAM has been formulated [24].

The so called "Flux-Based Methods Of Characteristics" [22] (FB-MOC) were described in [8] for numerical solution of advection dominated transport equation on unstructured 2D/3D grids. These methods are a straightforward extension of (vertex-centred aligned) finite volume methods to have no CFL condition for time steps.

In this paper, we present a general concept of FB-MOC. We define an analytical flux-based integral formulation of advection equation that involves the tracking of characteristic curves. For numerical approximation of such formulation we follow the basic property of finite volume discretization schemes - only transport between neighbour cells through common boundaries can occur during one time step. Applying such concept, the FB-MOC can be derived from a wide class of high-resolution FVM.

* This work is funded by the Federal Ministry of Economy and Technology (BMWi) under the contract number 02 E 9148 2

Using the analytical flux-based integral formulation, discretization schemes based on standard second order methods can be constructed by introducing a time step dependency of numerical solution in the approximation of advective fluxes. This can be realised by defining the so called "critical time steps" for each computational cell. The CFL condition is then given by minimal critical time step.

For such extensions of finite volume discretization schemes one can find sufficient conditions to prove the discrete minimum and maximum principle of numerical solution. Based on these conditions, an appropriate limiter can be constructed that is defined only locally and that can be viewed as a "minimal" modification of origin scheme to obtain the min-max principle.

One of such obtained discretization scheme coincides for one-dimensional case with Lax-Wendroff method using slope limiter, see e.g. [18] for its description. In this form, the method can be extended rather straightforwardly for larger time steps, see [22] for one-dimensional case. Following the approach of [8], we present analogous extension for general (unstructured) computational grids in R^2 or R^3.

Finally, the FB-MOC based on critical time step formulation can reduce significantly time splitting error if used within operator splitting methods. This is a crucial property for successful computations of coupled transport equations with different sorption kinetics. There, the effective advective velocity is different for each component of the system due to different retardation of the transport. Using classical operator splitting methods with large time step τ, a large error of order $O(\tau)$ is introduced. The approach described in this paper can reduce this error to be proportional locally to critical time steps.

The paper is organised as follows. In Section 2 we describe briefly mathematical model. In Section 3 the analytical flux-based integral formulation of advection equation is introduced. In Section 4 high-resolution finite volume methods based on analytical flux-based formulation are described. In Section 5 the discrete minimum and maximum principle for numerical solutions is proved. In Section 6 the Flux-Based Methods of Characteristics with no restriction on choice of time steps is derived. The standard operator splitting approach is described in Section 7. The FB-MOC for coupled system of transport equations is given in Section 8. Finally, some numerical experiments are presented in Section 9, and conclusions are summarised in Section 10.

2 Mathematical model

Let us consider several radioactive contaminants that are transported by groundwater flow with given velocity $\mathbf{v} = \mathbf{v}(x)$. Concentration of the r-th component at some time t and at some point x of a domain $\Omega \subset R^d$ will be denoted by $c^r = c^r(t,x)$.

The system is coupled through linear decay reactions (degradations), where the decay (sink) $\lambda^{rs}c^r$ of c^r represents a source to the component c^s. We consider here only constant reaction rates λ^{rs} . Moreover, each c^s can have only one source term $\lambda^{rs}c^r$.

Further, each contaminant can occur not only dissolved in flowing groundwater, but also adsorbed (immobilised) to the skeleton of porous media. If sorption reactions are fast enough (i.e. in an equilibrium), the total mass of contaminant c^r at some fixed time can be written as the sum of dissolved and adsorbed part, i.e.

$$\int_\Omega R^r \phi\, c^r dx = \int_\Omega \phi\, c^r dx + \int_\Omega (R^r - 1)\phi\, c^r dx\,.$$

The function $\phi = \phi(x)$ denotes the porosity of the medium, and $R^r = R^r(x) \geq 1$ are the retardation factors.

Finally, considering dispersive and diffusive transport of contaminants described by a diffusion-dispersion tensor D, one ends with the following system of equations,

$$R^r\phi\,\partial_t c^r + \nabla\cdot(\mathbf{v}c^r - D^r\nabla c^r) + \lambda^{rs}R^r\phi\, c^r = \lambda^{pr}R^p\phi\, c^p. \tag{1}$$

The values of $c^r(0,x)$ are prescribed by initial conditions. Moreover, we consider standard inflow/outflow boundary conditions

$$\mathbf{n}\cdot(\mathbf{v}c^r - D^r\nabla c^r) = \mathbf{n}\cdot\mathbf{v}C^r, \quad t \geq 0\,, \quad \gamma \in \partial\Omega\,, \tag{2}$$

where at the inflow part $\partial^{in}\Omega$ of boundary $\partial\Omega$, i.e. $\mathbf{n}(\gamma)\cdot\mathbf{v}(\gamma) < 0$ for $\gamma \in \partial^{in}\Omega \subset \partial\Omega$, the values of $C^r(t,\gamma)$ are given, otherwise $C^r(t,\gamma) \equiv c^r(t,\gamma)$.

The vector $\mathbf{n}$ denotes the normal outward unit vector with respect to Ω.

3 Analytical flux-based integral formulation

Any numerical method that aims to solve advection dominated transport equations, must be capable of solving the simple case of (1) - a linear advection equation

$$\partial_t c + \mathbf{v}\cdot\nabla c = 0 \tag{3}$$

with divergence free velocity field

$$\nabla\cdot\mathbf{v}(x) = 0\,, \quad x \in \Omega\,. \tag{4}$$

We describe Flux-Based Methods Of Characteristics for (3) - (4) and postpone the description of details for general form of (1). Due to the same reason, we consider only trivial homogeneous inflow boundary conditions, i.e. $C^r \equiv 0$, for treatment of general case see [8,9].

Of course, the problem (3) can be solved exactly. If $c(t^n,x)$, $x \in \Omega$ is known for t^n, then

$$c(t,x) = c(t^n, X(t^n;x,t)) \tag{5}$$

is the solution of (3) for $t \geq t^n$, where the point $X(t^n;x,t)$ is obtained by tracking backward the characteristic curve that starts at t in x and ends at t^n in X, i.e.

$$X(t^n;x,t) = x - \int_{t^n}^{t} \mathbf{v}(X(s;x,t))ds\,. \tag{6}$$

In general, $X(t^n;x,t)$ can lie outside of the domain Ω if the characteristic curve intersects the inflow boundary

$\partial^{in}\Omega$. In such a case, due to our trivial inflow boundary conditions, $c(t,x)=0$ in (5).

Our aim is to develop numerical methods with a clear form of local and global mass balance property. To derive it, we rewrite the differential equation (3) to an equivalent integral form that we present directly in the framework of Finite Volume Methods (FVM), i.e.

$$\int_{\Omega_i} c(t)\,dx = \int_{\Omega_i} c(t^n)\,dx - \int_{\partial\Omega_i} \mathbf{n}\cdot\mathbf{v}\int_{t^n}^{t} c(s)\,ds d\gamma\,. \tag{7}$$

In (7), $\Omega_i \subset \Omega$ for $i=1,\ldots,I$ are non-intersecting non-empty polygonal computational cells ("finite volumes") that cover the whole domain Ω. Moreover, we have skipped x argument of space dependent functions in (7).

Further, we denote

$$\Gamma_{ij} := \partial\Omega_i \cap \partial\Omega_j\,, \tag{8}$$

where it is enough to consider (8) only for Ω_j having "non-trivial" intersection with Ω_i, i.e. lines in two-dimensional (2D) case or polygons in 3D case, see for instance [7] for details.

Finally, $\mathbf{n}_{ij}$ denotes a constant normal vector associated with Γ_{ij} that points from Ω_i to Ω_j. Now, one can rewrite (7) to

$$\int_{\Omega_i} c(t)\,dx = \int_{\Omega_i} c(t^n)\,dx - \tag{9}$$

$$\sum_{j\in out(i)} \mathbf{n}_{ij}\cdot\int_{\Gamma_{ij}}\mathbf{v}\int_{t^n}^{t} c(s)\,ds d\gamma +$$

$$\sum_{k\in in(i)} \mathbf{n}_{ki}\cdot\int_{\Gamma_{ki}}\mathbf{v}\int_{t^n}^{t} c(s)\,ds d\gamma\ ,$$

where the sets $out(i)$ and $in(i)$ of indices are given by

$$j\in out(i) \text{ if } \int_{\Gamma_{ij}} \mathbf{n}_{ij}\cdot\mathbf{v}\,d\gamma > 0\,,$$

and $k\in in(i)$ if $i\in out(k)$.

Next, we introduce notations for time dependent averaged concentrations $c_i = c_i(t)$ in Ω_i,

$$c_i(t) := \frac{1}{V_i}\int_{\Omega_i} c(t,x)dx\,, \tag{10}$$

where $V_i := |\Omega_i|$, and, finally, we define the mass sources and sinks $m_{ij}^n = m_{ij}^n(t)$ at Γ_{ij} for $j\in out(i)$,

$$m_{ij}^n(t) := \mathbf{n}_{ij}\cdot\int_{\Gamma_{ij}}\mathbf{v}(\gamma)\int_{t^n}^{t} c(s,\gamma)\,ds d\gamma\,. \tag{11}$$

The equations (9) can be written now in the following simple form,

$$c_i(t)V_i = c_i(t^n)V_i - \sum_{j\in out(i)} m_{ij}^n(t) + \sum_{k\in in(i)} m_{ki}^n(t)\,. \tag{12}$$

The equality (12) expresses clearly the mass conservation principle. It states that the initial mass $c_i(t^n)V_i$ in Ω_i can change only due to mass sinks $m_{ij}^n(t)$ at outflow boundaries and mass sources $m_{ki}^n(t)$ at inflow boundaries of $\partial\Omega_i$.

An analytical integral formulation of Flux-Based Methods Of Characteristics (FB-MOC) involves definition of $m_{ij}^n(t)$ using characteristic curves (6), i.e.

$$m_{ij}^n(t) = \mathbf{n}_{ij}\cdot\int_{\Gamma_{ij}}\mathbf{v}(\gamma)\int_{t^n}^{t} c(t^n, X(s;\gamma,t))\,ds d\gamma\,. \tag{13}$$

The formulation (12), together with (13) and (6), was used for the description of "flux-based modified method of characteristics" for one-dimensional problems [22]. The simplicity of one-dimensional case of advection equation (3) enables to compute (12) for arbitrary large times, see [22] for all details.

Concerning several dimensional cases, i.e. $x\in R^2$ or R^3, it is in general too complicated to realise computations of (13) exactly. Especially for general unstructured grids, some numerical approximation of $m_{ij}^n(t)$ must be considered.

In following sections we present such formulations of Flux-Based Method Of Characteristics.

Remark 3.1. Of course, the "only" result of the exact computation of integral formulation for a particular finite volumes mesh is a piecewise constant approximation (10) of $c(t^{n+1},x)$. If such approximation is used also for computations of next time step, a significant interpolation error is introduced. High-resolution finite volume methods [18] that aim to reduce such error, will be discussed in the next section.

4 Finite volume discretization

Many discretization schemes of Finite Volume Methods (FVM) for purely advection equation (3) can be written in the following form,

$$c_i^{n+1}V_i = c_i^n V_i - \tau^n \sum_{j\in out(i)} c_{ij}^n v_{ij} + \tau^n \sum_{k\in in(i)} c_{ki}^n v_{ki}\,, \tag{14}$$

where $\tau^n := t^{n+1}-t^n$, and v_{ij} denotes the integrated flux over Γ_{ij},

$$v_{ij} := \mathbf{n}_{ij}\cdot\int_{\Gamma_{ij}}\mathbf{v}(\gamma)\,d\gamma\,.$$

Of course, $v_{ji} = -v_{ij}$.

If $c_i^n := c_i(t^n)$, see (10), then $c_i^n V_i$ denotes the exact amount of mass in Ω_i at $t=t^n$. Different discretization schemes are recognised by different choices of c_{ij}^n in (14).

4.1 The first order discretization scheme

The simplest particular form of (14) is the so called explicit "upwind" or "upstream" scheme,

$$c_i^{n+1}V_i = c_i^n\,(V_i - \tau^n v_i) + \tau^n \sum_{k\in in(i)} c_k^n v_{ki}\,, \tag{15}$$

where v_i denotes the integrated flux over $\partial^{out}\Omega_i$, i.e.

$$v_i := \sum_{j \in out(i)} v_{ij} \,.$$

This means, particularly, that for Γ_{ij} the values c_{ij}^n in (14) are determined with respect to the sign of v_{ij}, i.e. $c_{ij}^n \equiv c_i^n$ if $v_{ij} > 0$, and $c_{ij}^n \equiv c_j^n$ if $v_{ij} < 0$.

It is clear that (15) is feasible only if τ^n fulfills the CFL condition that can be written in the form

$$\tau^n \le \tau_{\rm CFL} := \min\{\tau_i, i = 1, \ldots, I\} \,, \tag{16}$$

where τ_i is the "critical time step" [8] for Ω_i,

$$\tau_i := \frac{V_i}{v_i} \,, \tag{17}$$

In practice, the search for the minimum in (16) can be restricted only to indices i with $c_i^n > 0$.

If (16) is not fulfilled then coefficients in (15) after c_i^n can become negative and nonphysical behaviour of numerical solutions can be expected, see Section 5 later.

Comparing (15) and (12), the explicit upwind scheme can be viewed as the approximation of $m_{ij}^n(t)$ in (13) by piecewise linear function in time, i.e.

$$m_{ij}^n(t) \approx (t - t^n)\, c_i^n\, v_{ij} \quad \text{ for } t \in [t^n, t^n + \tau_{\rm CFL}] \,. \tag{18}$$

For piecewise constant form of $c(t^n, x)$ and for one-dimensional case, the scheme (18) is the exact realisation of (12). This is a simple consequence of the fact that because of (4), $\mathbf{v} = v = const$, and the point $X(t^n; \gamma, t)$, that is tracked backwards from the point $\gamma \in \partial^{out}\Omega_i$, remains for $t \in (t^n, t^n + \tau_{\rm CFL})$ in Ω_i. Consequently, $c(t, X(t^n; \gamma, t)) \equiv c_i^n$.

For larger time steps this point will cross the inflow boundary of Ω_i, and the scheme (18) is no more appropriate. Extensions of (18) for larger time steps will be described in Section 6 .

4.2 High-resolution discretization schemes

Large class of higher order (or "high-resolution") explicit FVM schemes [18]) tries to replace the piecewise constant interpolation form of the first order scheme (that is clearly the main source of numerical error of this method [22,18]) by some more appropriate form.

The simplest method how to "reconstruct" such interpolation form is to interpolate linearly between values c_i and c_j. Particularly, the values c_{ij}^n in (14) can be determined by some convex combinations for $\alpha_{ij} \in [0, 1]$,

$$c_{ij}^n = (1 - \alpha_{ij}) c_i^n + \alpha_{ij} c_j^n \,. \tag{19}$$

If for each Ω_i a representative geometric point $x_i \in \Omega_i$ is defined, i.e. $c_i^n :\approx c(t^n, x_i)$, then the parameter α_{ij} can be determined from the position of intersection point $x_{ij} \in \Gamma_{ij}$ on the line between x_i and x_j. Of course, such intersection point $x_{ij} \in \Gamma_{ij}$ does not exist for arbitrary shape of Ω_i.

Another possibility (with no geometric restrictions) is to define some approximation $\tilde{\nabla} c_i^n$ of $\nabla c(t^n, x)$ per each Ω_i. This is a typical approach of "reconstruction methods", see [26,18,8]. In such a case, the value c_{ij}^n can be determined by

$$c_{ij}^n := c_i^n + \tilde{\nabla} c_i^n(x_{ij}) \cdot (x_{ij} - x_i) \,. \tag{20}$$

Our next considerations are applicable to any particular form of (14).

The first order discretization scheme can be viewed as an approximation of m_{ij}^n for piecewise constant form in space of $c(t^n, x)$ that results in a piecewise linear form in time of m_{ij}^n.

If $c(t^n, x)$ has a piecewise linear form like (19) or (20) then $c(t^n, X(t^n; \gamma, t))$ might vary (piecewise) linearly in time. From this point of view, the following piecewise quadratic approximation of $m_{ij}^n(t)$ can be derived,

$$m_{ij}^n(t) \approx (t - t^n) \left(c_{ij}^n + \frac{t - t^n}{\tau_i} \left(c_i^n - c_{ij}^n \right) \right) v_{ij} \,. \tag{21}$$

For one dimensional case, (21) can be viewed as an exact realisation of (13) for piecewise linear form of $c(t^n, x)$.

Using (21), the standard discretization scheme (14) can be replaced by the "time step depending form",

$$\begin{aligned} c_i^{n+1} V_i = c_i^n V_i - \tau^n \sum_{j \in out(i)} c_{ij}^n(\tau^n)\, v_{ij} + \\ + \tau^n \sum_{k \in in(i)} c_{ki}^n(\tau^n)\, v_{ki} \end{aligned} \tag{22}$$

that is valid for $\tau^n \le \tau_{\rm CFL}$, and where

$$c_{ij}^n(\tau^n) := c_{ij}^n + \frac{\tau^n}{\tau_i}(c_i^n - c_{ij}^n) \,.$$

Analogous extensions of (14) can be realised even for more complex interpolations of $c(t^n, x)$, but the property $c_{ij}^n(\tau_i) = c_i^n$ should be always fulfilled.

The scheme (22) coincides for one dimensional case with Lax-Wendroff scheme, compare (22), for instance, with description in [18].

In the following section, under some assumptions, we prove the local minimum and maximum principle for c_i^{n+1} in (22). To fulfill such assumptions in general, the "slope limiter" method might be applied that replace c_{ij}^n by some "limited" value $\bar{c}_{ij}^n \in [c_i^n, c_{ij}^n]$.

5 Discrete minimum and maximum principle

Formally, discretization schemes (14) takes the form

$$\beta_{ii} c_i^{n+1} = \sum_k \beta_{ik} u_{ik}^n \,, \tag{23}$$

where k runs through indices of some finite subset of $\{1, \ldots, I\}$, and u_{ik}^n are some known values.

The following Lemma states a "local" discrete minimum and maximum principle for c_i^{n+1}.

Lemma 5.1. *Let parameters β_{ii} and β_{ik} in (23) fulfill*

$$\beta_{ii} > 0 \,, \quad \beta_{ik} \ge 0 \,, \quad \beta_{ii} = \sum_k \beta_{ik} \,.$$

Moreover, let values u_{ik}^n be bounded by

$$\min_k\{c_k^n\} \le u_{ik}^n \le \max_k\{c_k^n\}\,.$$

Then the following local minimum and maximum principle is valid for c_i^{n+1},

$$\min_k\{c_k^n\} \le c_i^{n+1} \le \max_k\{c_k^n\}\,. \tag{24}$$

The Lemma 5.1 is a special case of even more general results, see for instance [15,6].

For the first order scheme (15), the assumptions of Lemma 5.1 are clearly fulfilled if the CFL condition (16) is valid. Particularly, the estimates (24) take the form

$$c_{i,min}^n \le c_i^{n+1} \le c_{i,max}^n\,, \tag{25}$$

$$c_{i,min}^n := \min\{c_i^n\,,\, \min_{k\in in(i)}\{c_k^n\}\}\,,$$

$$c_{i,max}^n := \max\{c_i^n,\, \max_{k\in in(i)}\{c_k^n\}\}\,.$$

For high-resolution schemes (22) the discrete minimum and maximum principle can be proved under certain additional assumptions.

Theorem 5.1. *Let (16) be valid and let c_{ki}^n, $k \in in(i)$ and c_{ij}^n, $j \in out(i)$ in (14) fulfill*

$$c_{i,min}^n \le c_{ki}^n \le c_{i,max}^n\,, \tag{26}$$

$$2c_i^n - c_{i,max}^n \le c_{ij}^n \le 2c_i^n - c_{i,min}^n\,. \tag{27}$$

Then c_i^{n+1} in (22) fulfills the local discrete minimum and maximum principle (25).

Proof. Let $c_{ij}^n \ge c_i^n$. Then, due to (27), there exists $\alpha_{ij}^n \in [1,2]$ such that

$$c_{ij}^n = \alpha_{ij}^n c_i^n - (\alpha_{ij}^n - 1)c_{i,min}^n\,.$$

Analogous properties can be obtained if $c_{ij}^n \le c_i^n$,

$$c_{ij}^n = \alpha_{ij}^n c_i^n - (\alpha_{ij}^n - 1)c_{i,max}^n\,.$$

Substituting c_{ij}^n into (22) and using (17), one obtains

$$\begin{aligned} c_i^{n+1}V_i = \quad & \\ c_i^n \sum_{j\in out(i)} v_{ij}\left(\tau_i - \tau^n\left(\alpha_{ij}^n + \frac{\tau^n}{\tau_i}(1-\alpha_{ij}^n)\right)\right) + & \\ + \tau^n(1-\frac{\tau^n}{\tau_i})\sum_{j\in out(i)} c_{i,*}^n v_{ij}(\alpha_{ij}^n - 1) + & \\ + \tau^n \sum_{k\in in(i)} v_{ki}\left(c_{ki}^n + \frac{\tau^n}{\tau_k}(c_k^n - c_{ki}^n)\right)\,, & \end{aligned} \tag{28}$$

where $c_{i,*}^n = c_{i,min}^n$ if $c_{ij}^n > c_i^n$, and $c_{i,*}^n = c_{i,max}^n$ if $c_{ij}^n < c_i^n$ (for $c_{ij}^n = c_i^n$ one takes simply $c_{i,*}^n = c_i^n$). Using

$$\tau_i - \tau^n\left(\alpha_{ij}^n + \frac{\tau^n}{\tau_i}(1-\alpha_{ij}^n)\right) =$$

$$(\tau_i - \tau^n)\left(1 - (\alpha_{ij}^n - 1)\frac{\tau^n}{\tau_i}\right) \ge 0\,,$$

the assumptions of Lemma 5.1 are fulfilled.□

Remark 5.1. For (19), (26) is trivially fulfilled. For (20), the origin values c_{ki}^n of (14) must be replaced by the "limited" values $\bar{c}_{ki}^n$,

$$\bar{c}_{ki}^n := \begin{cases} c_{i,min}^n & c_{ki}^n < c_{i,min}^n \\ c_{ki}^n & c_{i,min}^n \le c_{ki}^n \le c_{i,max}^n \\ c_{i,max}^n & c_{i,max}^n < c_{ki}^n \end{cases}\,. \tag{29}$$

Similarly, the assumptions (27) are not fulfilled in general. Nevertheless, they give straightforward hint how to limit c_{ij}^n if necessary.

For instance, if $c_{i,min}^n + c_{ij}^n > 2c_i^n$ then c_{ij}^n in (22) must be replaced by $\bar{c}_{ij}^n := 2c_i^n - c_{i,min}^n$. In an extreme case, if for instance $c_i^n = c_{i,min}^n$, the value c_{ij}^n must be replaced by c_i^n, and, consequently, the first order scheme must be applied locally at Γ_{ij}.

6 The FB-MOC without CFL condition

In this section, we describe the simplest variant of the Flux-Based Method Of Characteristics (FB-MOC). The idea is to extend any numerical approximation of $m_{ij}^n(t)$ from (13), e.g. (18) or (21), for time steps τ^n that do not fulfil the CFL condition (16). The algorithm, presented here, is based on the first order scheme (15), but, as we show later, it can be used successfully for any approximation of $m_{ij}^n(t)$. We remind that the function $m_{ij}^n(t)$ in (13) describes how much mass is transported in time interval (t^n, t) through $\Gamma_{ij} \subset \partial_i^{out}\Omega_i$.

In the following Remark we describe two properties of discretization scheme (15) that will be used in the general implementation of FB-MOC. In fact, the next Remark describes the only approximations that are used in the realization of FB-MOC.

Remark 6.1. For the approximation of $m_{ij}^n(t)$ in (13) the following two assumptions must be valid:

1. arbitrary fraction of mass that starts to flow into Ω_i at time t, can start to leave it only at time $t + \tau_i$;
2. such fraction of mass is transported proportionally through entire outflow boundary $\partial^{out}\Omega_i$.

We discuss both assumptions in details. To do so, we rewrite (15) to an equivalent form,

$$\begin{aligned} c_i^{n+1}V_i = c_i^n V_i - \sum_{j\in out(i)}\left(\frac{\tau^n}{\tau_i}\frac{v_{ij}}{v_i}\right)c_i^n V_i + & \\ \sum_{k\in in(i)}\left(\frac{\tau^n}{\tau_k}\frac{v_{ki}}{v_k}\right)c_k^n V_k\,. & \end{aligned} \tag{30}$$

The discretization scheme (30) fulfills clearly both assumptions of the Remark 6.1.

Firstly, it assumes that only fractions of mass $c_i^n V_i$ are transported from Ω_i to neighbours Ω_j, $j \in out(i)$. The fractions of $c_k^n V_k$, $k \in in(i)$, that enter Ω_i from Ω_k, remain in Ω_i during this time interval.

Considering the analytical description (13), this is clearly only approximation of an exact situation in general. Flow particles that enter Ω_i, for instance, through

$\Gamma_{ki} \subset \partial^{in}\Omega_i$ during $(t^n, t^n+\tau_i)$ may also leave Ω_i in this time interval, and, consequently, the same must be valid for corresponding fractions of $c_k^n V_k$.

Secondly, the second assumption of Remark 6.1 is fulfilled for (30). The mass $c_i^n V_i$ (that can be viewed as a sum of fractions of $c_k^{n-1}V_k$ from inflow contributions to Ω_i in previous time step) is transported proportionally to all Ω_j for $j \in out(i)$.

In general, this assumption is only approximation of the analytical description (13). For example, all flow particles that enter Ω_i through a particular $\Gamma_{ki} \subset \partial^{in}\Omega_i$, may leave Ω_i only through a single $\Gamma_{ij} \subset \partial^{out}\Omega_i$. Consequently, the corresponding fraction of $c_k^n V_k$ is transported further only to one neighbour cell Ω_j.

Using the assumptions (or approximations) of Remark 6.1, it is now straightforward to extend (15) or (22) for larger time steps.

First of all, due to our trivial boundary conditions and the presence of no source terms in (3), the mass $c_i(t)V_i$ in Ω_i for $t \in [t^n, t^{n+1}]$ can be expressed in the form [8],

$$c_i(t)V_i = \sum_{k=1}^{I} c_k^n V_k \, \delta_{ki}^n(t)\,, \tag{31}$$

where $0 \le \delta_{ki}^n(t) \le 1$. Our aim is to compute $\delta_{ki}^n(t)$ in (31) for $t = t^{n+1}$ only approximately. In such a way, let $\delta_{ki}^{n+1} :\approx \delta_{ki}^n(t^{n+1})$, and we consider the following discretization scheme,

$$c_i^{n+1}V_i = \sum_{k=1}^{I} c_k^n V_k \, \delta_{ki}^{n+1}\,. \tag{32}$$

We first derive the right hand side of (32) for time steps that fulfills the CFL condition (16). Using the first assumption of Remark 6.1, one obtains

$$c_k^n V_k = \sum_{i \in out(k)} m_{ki}^n(t^n + \tau_k)\,. \tag{33}$$

Considering now arbitrary $m_{ki}^n(t)$, that fulfill $m_{ki}^n(t^n) = 0$ and (33), one can define

$$\delta_{ki}^n(t) := \frac{m_{ki}^n(t)}{c_k^n V_k}\,, \quad \delta_{ii}^n(t) := 1 - \sum_{j \in out(i)} \delta_{ij}^n(t)\,, \tag{34}$$

and, consequently, the scheme (32) can be written for $t^{n+1} \le t^n + \tau_{\rm CFL}$ in the form

$$c_i^{n+1}V_i = c_i^n V_i \, \delta_{ii}^{n+1} + \sum_{k \in in(i)} c_k^n V_k \, \delta_{ki}^{n+1}\,. \tag{35}$$

We describe the FB-MOC by extending the definitions of $\delta_{ki}^n(t)$ in (32) for $t > t^n + \tau_{\rm CFL}$. To do so, we use strictly only the two assumptions that are defined in the Remark 6.1.

We introduce here the so called "forward tracking" variant of FB-MOC. Concretely, if $m_{ki}^n(t)$ describes the mass that is flowing through Γ_{ki} for $t \in (t^n, t^n+\tau_k)$, we follow this mass further for all Γ_{ij}, $j \in out(i)$, and for $t \in (t^n+\tau_k, t^{n+1})$.

In such a way, this algorithm can compute for each initial mass $c_k^n V_k$, $k = 1, \ldots, I$ all nonzero values of δ_{ki}^{n+1} in (32). For the particular approximation of m_{ki}^n defined by (18), this algorithm was described in [8].

Unfortunately, it is too complicated to find a straightforward definition of δ_{ki}^{n+1}. In general, this value must be defined as a sum of several "partial" fractions, because several fractions of $c_k^n V_k$ may arrive from Ω_k to Ω_i through different pathes. Such an alternative description of the FB-MOC is in preparation [12].

In this paper we introduce a recursive procedure how to compute δ_{ki}^{n+1} for a fixed k. Initially, we set $\delta_{ki}^{n+1} = 0$ for $i = 1, \ldots, I$ and in the next algorithm we update (possibly several times) these values by adding some "partial fractions" to them, see (36) and (37) later.

Let the function $m_k = m_k(t)$ denotes some arbitrary (time dependent) fraction of $c_k^n V_k$, i.e. $m_k(t) \le c_k^n V_k$, that flows into some Ω_i during time interval $[t_1, t_2] \subset [t^n, t^{n+1}]$. At the beginning of this recursive algorithm, one has to start with $m_k(t) = m_{ki}^n(t)$ for all $i \in out(k)$ with $t_1 = t^n$ and $t_2 = \min\{t^n + \tau_k, t^{n+1}\}$.

Of course, $m_k(t_1) = 0$ and $m_k(t)$ must be a nondecreasing function in time. This means that m_k takes the maximal value at $t = t_2$ and we suppose that $m_k(t_2) > 0$. To decide, if this mass $m_k(t_2)$ (or some fraction of it) remains in Ω_i (i.e. that the value δ_{ki}^{n+1} has to be updated), we discuss three possible situations.

In the first situation, one has to consider the case $t_1 + \tau_i \ge t^{n+1}$. In this case, due to the first assumption in Remark 6.1, the mass $m_k(t_2)$ remains in Ω_i completely, i.e.

$$\delta_{ki}^{n+1} += \frac{m_k(t_2)}{c_k^n V_k}\,, \tag{36}$$

where $a+=b$ should be understood as in programming languages, i.e. 'add b to a".

In the second situation, one has to consider $t_1 + \tau_i < t^{n+1}$ and $t_2 + \tau_i \le t^{n+1}$. In such a case, the mass $m_k(t_2)$ will leave Ω_i completely, so no update of δ_{ki}^{n+1}, for this moment, is necessary. Due to the second assumption of the Remark 6.1, this recursive algorithm will be now considered for functions $m_j = m_j(t)$ and computational cells Ω_j, $j \in out(i)$, where

$$m_j(t) := \frac{v_{ij}}{v_i}\, m_k(t - \tau_i),\ t \in (t_1 + \tau_i, t_2 + \tau_i).$$

Finally, in the third situation, one has to consider $t_1 + \tau_i < t^{n+1}$ and $t_2 + \tau_i > t^{n+1}$. In this case, the mass $m_k(t_2) - m_k(t^{n+1} - \tau_i)$, that entered Ω_i during time interval $(t^{n+1} - \tau_i, t_2)$, remains in Ω_i, and the rest must be considered further with this algorithm. Particularly, the value δ_{ki}^{n+1} must be updated as follows,

$$\delta_{ki}^{n+1} += \frac{m_k(t_2) - m_k(t^{n+1} - \tau_i)}{c_k^n V_k}\,, \tag{37}$$

(see the explanation of $a+=b$ before), and this recursive algorithm must be now considered for functions $m_j = m_j(t)$ and computational cells Ω_j, $j \in out(i)$, where

$$m_j(t) := \frac{v_{ij}}{v_i}\, m_k(t - \tau_i),\ t \in (t_1 + \tau_i, t^{n+1}).$$

It is clear that starting with $\delta_{ki}^{n+1} = 0$, $i = 1, \ldots, I$, $i \ne k$, and $m_k(t) = m_{kj}^n(t)$ from (21) for Ω_j, $j \in out(k)$,

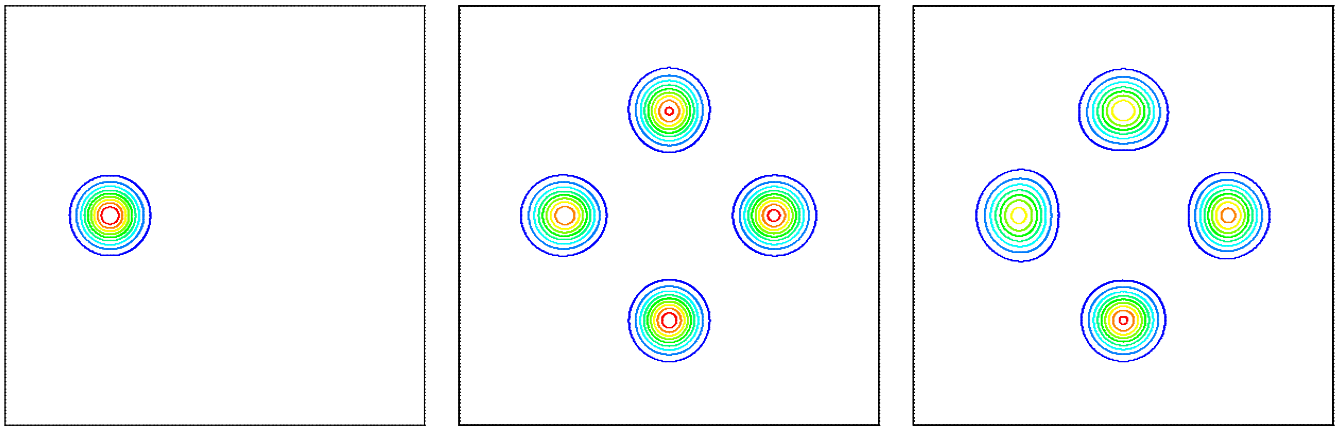

Fig. 1. The initial function $c^0(x)$ of Example 6.1 (left picture), numerical solution at $t = \pi/8, \pi/4, 3\pi/8$ and $\pi/2$ for $\tau = \pi/2/M$ with $M = 128$ (middle picture), and analogous numerical solution for $M = 1024$ (right picture).

$t_1 = t^n$, $t_2 = t^n + \min\{t^{n+1}, t^n + \tau_k\}$, this algorithm must finish for all $k = 1, \ldots, I$ in a finite number of recursive steps.

The values δ_{kk}^{n+1} are defined for $t \in (t^n, t^n + \tau_k)$ analogously to (34), particularly, $\delta_{kk}^n(t^n + \tau_k) = 0$. For $t > t^n + \tau_k$ the previous recursive algorithm applies also to δ_{kk}^{n+1}. Finally, the treatment of outflow boundary conditions for FB-MOC can be found in [8,9].

Example 6.1. The well-known test example of rotating Gaussian impulse with no diffusion was tested with FB-MOC based on the first order discretization scheme (15) on triangular mesh. The implementation was realised with software library *UG* [1].

The (divergence free) velocity is chosen such that the initial profile of exact solution rotates anticlockwise, and it returns unchanged to the origin position at $t = \pi/2$, see the left picture in the Figure 1.

The time step $\tau = \pi/2/M$ is determined by the choice of M. The initial grid consisted of 8 right triangles Ω_i (i.e. $I = 8$ for the "grid level" 0). This grid was 8 times uniformly refined, it means that each triangle was regularly divided into 4 subtriangles for one uniform refinement.

The plot of the numerical solution at the grid level 8 (524288 triangles) can be seen in the Figure 1, the middle picture, for $M = 128$. The 9 contour lines correspond to values $0.1, \ldots, 0.9$.

The choice $M = 128$ corresponds to "grid Courant number" equals 25, i.e. some nonzero fraction of mass was transported over 25 computational cells in a single time step. The results for $M = 3200$, i.e. $\tau \approx \tau_{\text{CFL}}$, are plotted in the right picture of Figure 1. Clearly, the solution is corrupted by too many interpolations steps and it documents "strange" behaviour of FB-MOC based on the first order scheme (18), namely, that the method performs better for larger than for smaller time steps [23].

Numerical results for grid levels $l = 5, 6, 7$ and 8 are compared in the Table 1 with the discrete error E^l,

$$E^l := \sum_{i=1}^{I} V_i |c_i^M - c^{\text{exact}}(x_i, y_i, \pi/2)| \tag{38}$$

Table 1. Numerical convergence of FB-MOC.

l	M	$\max_{i=1,\ldots,I}\{c_i^M\}$	E^l	α^l
Exact	$t = \pi/2$	1.000	0.0	
5	16	0.526	6.254e-3	
6	32	0.683	3.826e-3	0.709
7	64	0.808	2.176e-3	0.814
8	128	0.892	1.173e-3	0.891
8	3200	0.744	2.843e-3	

and numerical convergence rates α^l,

$$\alpha^l := \frac{\log(E^l) - \log(E^{l-1})}{\log(0.5)}\,. \tag{39}$$

The results suggest, as expected, that numerical convergence rates α^l approaches 1 for FB-MOC.

Remark 6.2. Finite volume methods can be divided to two basic subclasses - the so called "cell-centred" and the "vertex-centred" methods.

The cell centred FVM use the primary mesh of "finite elements" Ω_i as the mesh of computational cells, and the corresponding averaged concentrations $c_i^n \approx c(t^n, x_i)$, $x_i \in \Omega_i$, are placed in the middles x_i of cells Ω_i.

The most important message of previous Example 6.1 is that for simple computational cells, i.e. with fewer boundary faces, the so called "grid effect" is negligible. In general, the grid effect is caused by the second approximation in Remark 6.1, and it can be recognised by an unphysical transversal dispersion of numerical solutions. Some possible reduction of grid effects for triangular finite element meshes in R^2 were discussed in [8].

On the other hand, the vertex-centred FVM are based on dual meshes that are constructed complementary to finite element meshes, see also "control volume finite element methods" [21] or "finite volume element methods" [4]. Consequently, the vertices of finite element triangulations lie in the middle of finite volume cells and standard finite element interpolation can be used for numerical approximation of $c(t^n, x)$ (and of $\nabla c(t^n, x)$).

The shapes of vertex-centred computational cells is complex in general. Nevertheless, a certain freedom for

their construction can be used to align some segments of $\partial\Omega_i$ to $\mathbf{v}$, see [16] for a description of "aligned finite volume methods".

All numerical experiments in next sections were realised using aligned FVM. Moreover, high resolution discretization scheme (22) based on (20) was used, where $\tilde{\nabla} c_i^n$ was computed by averaging the gradient of standard finite element interpolation, see also [26,20,11].

Finally, we note that another approach to reduce grid effects is to use "dimensional splitting" of $\mathbf{v}$, see e.g. [18,19], or the tracking of integration points instead of masses [13,14,25].

7 Operator splitting method

In previous sections we treated the Flux-Based Method of Characteristics (FB-MOC) for advection equations only. Our aim is to apply this method to general form of transport equation (1). In this section, we discuss briefly possible applications of FB-MOC using an operator splitting approach (or "fractional-step methods" [18]) .

In its "basic" form, the operator splitting approach consists of splitting the general transport operator to advective part and to the rest, and to solve each subproblem separately. The advantage of operator splitting methods is that each subproblem becomes simpler than the origin problem, and, formally, each equation can be solved by different numerical methods. The disadvantages is that a splitting error is introduced, independently of how good each equation is solved. This splitting error can vanish only for special cases, for instance if two corresponding operators commute, see e.g. [18].

The FB-MOC for advection-diffusion case of (1), using operator splitting approach, has been described in [8]. We skip the treatment of diffusion-dispersion here, and we treat in details only the system of coupled transport equations without diffusion-dispersion, i.e.

$$R^r \phi\, \partial_t c^r + \nabla \cdot (\mathbf{v}\, c^r) + \lambda^{rs} R^r \phi\, c^r = \lambda^{pr} R^p \phi\, c^p\,. \qquad (40)$$

Two subproblems, after operator splitting, take the form

$$R^r \phi\, \partial_t c^r + \nabla \cdot \mathbf{v} c^r = 0 \qquad (41)$$

and

$$R^r \partial_t c^r + \lambda^{rs} R^r c^r = \lambda^{pr} R^p c^p\,. \qquad (42)$$

The equations (42) can be solved exactly, see e.g. [5].

If all retardation factors R^r in (40) are identical, i.e. $R^r \equiv R$, then advection and reaction operators commute and there is no time splitting error for this operator splitting method.

Particularly, if the right hand side of (40) is zero, then, to solve (40), any method of characteristics can be extended straightforwardly - one has to replace the definition of $c(t,x)$ in (5) by

$$c^r(t,x) = c^r(t^n, X^r(t^n;x,t)) \exp(-\lambda^{rs}(t-t^n))\,, \qquad (43)$$

where

$$X^r(t^n;x,t) = x - \int_{t^n}^{t} \frac{\mathbf{v}(X^r(s;x,t))}{R^r(X^r(s;x,t)\phi(X^r(s;x,t))} ds. \qquad (44)$$

The difficulties arise for transport equation with some nonzero source term $\lambda^{pr} R^p c^p$ that moves with different effective velocity $\mathbf{v}/R^p\phi$ than the advection of c^r that moves with velocity given by $\mathbf{v}/R^r\phi$. This is illustrated clearly by the following simple example.

Example 7.1. Let us solve two equations,

$$\partial_t c^1 + \nabla \cdot \left(\mathbf{v} c^1\right) + \lambda c^1 = 0, \quad c^1(0,x) = c^0(x), \qquad (45)$$

$$\partial_t c^2 - \lambda c^1 = 0, \quad c^2(0,x) = 0,$$

where all data are given analogously as in Example 6.1. This problem can be viewed, formally, as a special case of (40) with $R_2 >> R_1$.

Clearly, the solution of (45) is $c^1 = c^0(X(t))e^{-\lambda t}$ and $c^2 = c^0(X(t))(1-e^{-\lambda t})$, where $X(t)$ is the characteristic curve corresponding to $\mathbf{v}$.

If the standard operator splitting approach is used with large time steps τ^n (i.e. the exact solution of (42) is found first, and afterwards, the transport (41) is solved), a large error of order $O(\tau^n)$ for c^2 is introduced even if the transport is solved exactly. This is clearly illustrated by the left picture of Figure 2, where the discrete steps of operator splitting method for a "coarse grid" are clearly visible.

On the other hand, if operator splitting approach is applied using critical time steps τ_i, see next section, the time splitting error is of order of maximal critical time step $\tau_{\max} := \max\{\tau_i; i = 1,\dots,I\}$, see the right picture of Figure 2.

8 FB-MOC for coupled transport equations

Firstly, we derive discretization scheme for coupled transport-reaction equations (40) using standard operator splitting method, i.e. the reaction equations (42) are solved exactly, and the advection equations (41) are solved by high-resolution finite volume methods.

To use properly the analytical solution of (42), let us define the following auxiliary problems for functions $\sigma_{p_0}^{p_k} = \sigma_{p_0}^{p_k}(t)$,

$$\frac{d}{dt}\sigma_{p_0}^{p_0} + \lambda^{(p_0 p_1)}\sigma_{p_0}^{p_0} = 0\,,$$
$$\frac{d}{dt}\sigma_{p_0}^{p_k} + \lambda^{p_k p_{k+1}}\sigma_{p_0}^{p_k} = \frac{R^{p_{k-1}}}{R^{p_k}}\lambda^{p_{k-1}p_k}\sigma_{p_0}^{p_{k-1}}\,, \qquad (46)$$

with initial values

$$\sigma_{p_0}^{p_0}(0) = 1\,, \quad \sigma_{p_0}^{p_k}(0) = 0\,,$$

where $\sigma_{p_0}^{p_0}$ is placed at the top of decay chain (i.e. no source in (42)), and k (or p_k) runs further through indices of all successors in the decay chain. If $R^r = R^r(x)$ then (46) must be solved for each Ω_i.

The exact solution of (46) can be found in several papers, see e.g. [5]. Of course, $\sigma_{p_0}^{p_0}(t) = e^{-\lambda^{p_0 p_1} t}$.

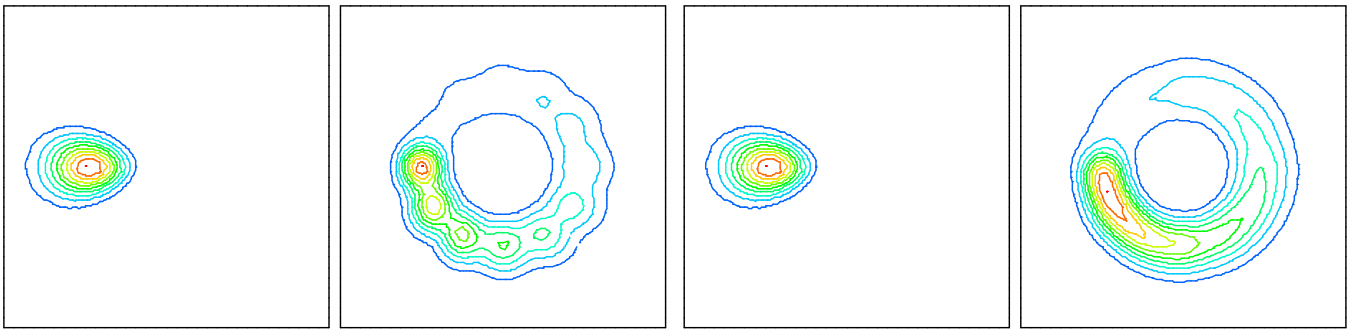

Fig. 2. Numerical solution c^1 and c^2 of Example 7.1 after 16 uniform time steps τ with standard operator splitting (the left two pictures, error of order $O(\tau)$ with $\tau >> \tau_{\mathrm{CFL}}$) and analogous numerical solution with application of algorithm in Section 8 (two right pictures, error of order $O(\tau_{\max})$ with $\tau_{\max}$ being maximal critical time step). Note that unsatisfactory numerical approximation of c^1 is due to coarse computational grid.

The discretization scheme for advection-reaction system (40) can be now written in the form

$$c_i^{r,n+1} R_i^r \phi_i V_i = \sum_p \sigma_p^r(\tau^n) \left(c_i^{p,n} R_i^p \phi_i V_i - \right. \tag{47}$$

$$\left. \tau^n \sum_{j \in out(i)} v_{ij}\, c_{ij}^{p,n}(\tau^n) + \tau^n \sum_{k \in in(i)} v_{ki}\, c_{ki}^{p,n}(\tau^n) \right) ,$$

where p starts with $p = r$, and it runs further through indices of all predecessors of c^r in the decay chain. The values ϕ_i represent averaged values of ϕ in Ω_i and, analogously, the values for R^r and R^p are defined.

The definition (17) of critical time step τ_i must be extended to τ_i^r,

$$\tau_i^r := \frac{R_i^r \phi_i V_i}{v_i} , \tag{48}$$

and the CFL condition (16) must be replaced for systems of equations by

$$\tau^n \le \tau_{\mathrm{CFL}}^{\mathrm{R}} := \min_i \min_r \tau_i^r . \tag{49}$$

An extension of (47) for larger time steps is analogous to (32) for single advection equation, i.e.

$$c_i(t) V_i = \sum_p \sum_{k=1}^{I} c_k^n V_k\, \delta_{ki}^{n,p}(t) , \tag{50}$$

where the index p runs, formally, over indices of all components of the system.

One can start again with an arbitrary function $m_k^r = m_k^r(t)$ and time interval (t_1, t_2) that describes how much fraction of mass of $c_k^r V_k$ enters some computation cell Ω_i^s, where the notation Ω_i^s emphasises that Ω_i is treated for c^s in (40). Additionally to the previous approach, one needs to register a time $t_{dec} \in (t^n, t^{n+1}]$ that denotes the next discrete time when the decay step of operator splitting procedure must be realised.

Initially, the function $m_k^r(t)$ is considered for each $j \in out(k)$, $k = 1, \ldots, I$ and for all indices p in the form,

$$m(t) = (t - t^n)\, v_{kj}\, c_{kj}^{p,n} (t - t^n)\, \sigma_p^r(t) ,$$

where $c_{kj}^{p,n}$ is defined analogously to (22), the index p starts with r and it runs through indices of all successors of decay chain. Further, $t_1 = t^n$, $t_2 = \min\{t^n + \tau_k^r, t^{n+1}\}$, $t_{dec} = \min\{t^n + \tau_k^p, t^{n+1}\}$.

The "distribution" of $m(t)$ is identical to the treatment in Section 6. Only if $t_{dec} < t^{n+1}$ then before continuing the transport to next neighbour cells at outflow, the decay step must be considered. There are several possibilities how to do this, and, formally, the partial transport step in algorithm of FB-MOC can be "interrupted" at any Ω_i^s for some time t where $t_{dec} \le t \le t_{dec} + \tau_i^s$. At this moment, the decay step must be realised, and the transport must continue with updated value of t_{dec}.

Such algorithm was realised in the software package R^3T (Retardation-Reaction-Radionuclides Transport), and more details will be published elsewhere.

9 Numerical experiments

To illustrate the behaviour of FB-MOC for coupled transport equations, two nontrivial examples are presented.

Example 9.1. To test the Flux-Based Method Of Characteristics for coupled transport equations with different retardation factors, we choose an extended version of rotated Gaussian impulse with three components:

$$R^1 \partial_t c^1 + \nabla \cdot \left(\mathbf{v} c^1 - \epsilon \nabla c^1 \right) + R^1 \lambda^{12} c^1 = 0 ,$$
$$R^2 \partial_t c^2 + \nabla \cdot \left(\mathbf{v} c^2 \right) + R^2 \lambda^{23} c^2 = R^1 \lambda^{12} c^1 ,$$
$$R^3 \partial_t c^3 + \nabla \cdot \left(\mathbf{v} c^3 \right) = R^2 \lambda^{23} c^2 ,$$

where $\mathbf{v} = 4(0.5 - y, x - 0.5)$, $R^1 = 1$, $R^2 = 2$, $R^3 = 4$, further $\lambda^{12} = 0.1$, $\lambda^{23} = 0.05$, and, finally, $\epsilon = 0.0001$.

The exact solution C^1 is known only for c^1,

$$C^1 = \frac{1}{1 + 10^3 t\, \epsilon} \exp\left(- \frac{(\tilde{x} + 0.25)^2 + \tilde{y}^2}{0.004 + 4t\epsilon} - \lambda_{12} t \right) , \tag{51}$$

where

$$\tilde{x} = (x - 0.5)\cos(4t) + (y - 0.5)\sin(4t) ,$$

$$\tilde{y} = (y - 0.5)\cos(4t) - (x - 0.5)\sin(4t).$$

The problem is solved on a square $(-1, -1) \times (1, 1)$ with trivial boundary conditions (2) (that are fulfilled by C^1

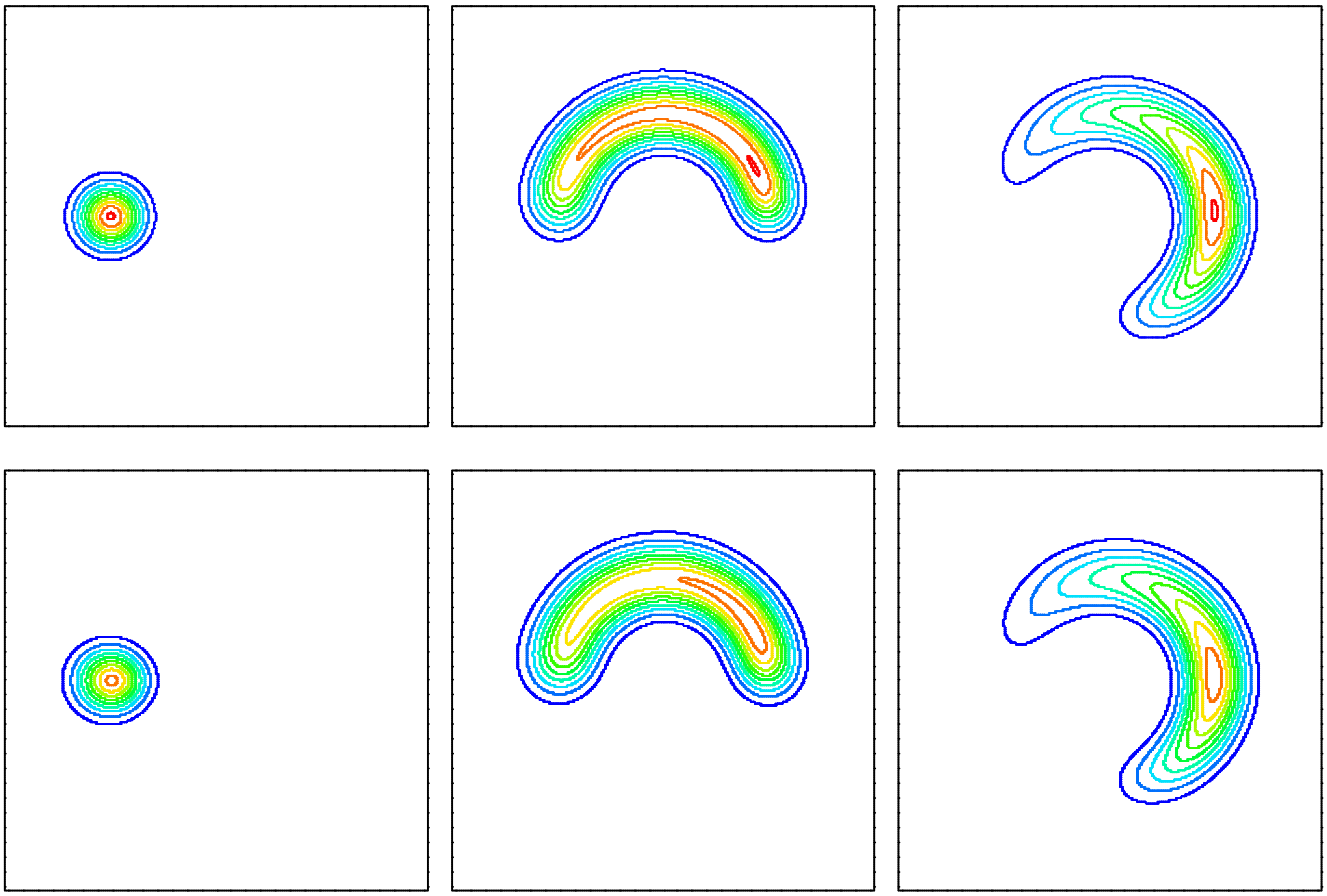

Fig. 3. Numerical solution of Example 9.1 at $t = \pi/2$ for $\tau = \pi/2/2048$ (top picture) and for $\tau = \pi/2/128$ (bottom picture).

only approximately). The initial condition for c^1 is taken from (51), the components c^2 and c^3 are initially zero.

The computations were realised with numerical library UG [1] using aligned vertex-centred dual mesh [16]. The second order discretization scheme (22) was used with limiter described after Theorem 5.1 and with FB-MOC described in section 8.

The initial grid ("grid level 0") consists of 4 triangles with single inner grid node $(0, 0)$. An uniform refinement is used to obtain next grid levels with each triangle from previous level divided regularly to 4 similar subtriangles.

Numerical solutions for c^1 are compared for different grid levels and different time steps $\tau := \pi/2/M$ in the Table 2, where the discrete errors E^l from (38) and the numerical convergence rates α^l from (39) are listed.

Table 2. Numerical results for Example 9.1

l	M	$C^1_{\max}$	$C^2_{\max}$	$C^3_{\max}$	$E^{1,l}$	$\alpha^{1,l}$
		0.739	?	?	0.0	
5	16	0.350	6.98e-3	1.79e-3	5.96e-3	
6	32	0.479	8.11e-3	2.08e-3	3.69e-3	0.692
7	64	0.580	8.96e-3	2.28e-3	2.14e-3	0.786
8	128	0.649	9.51e-3	2.40e-3	1.17e-3	0.870
8	384	0.648	9.63e-3	2.44e-3	1.17e-3	
8	2048	0.708	10.0e-3	2.53e-3	0.36e-3	

The Figure 3 shows numerical solutions on the grid level 8. The top picture shows all 3 components for $t = \pi/2$ that were obtained with $M = 2048$ that corresponds roughly to the Courant number τ/τ_{CFL} equals 1, i.e. the discretization scheme (47) with CFL condition was used. The bottom picture was obtained for $M = 128$ (Courant number ≈ 9). The equidistant contour lines for each component are the same for $M = 2048$ and for $M = 128$.

The numerical solution with CFL condition fulfilled approximates C^1 with the smallest error, but the computational time was the longest, it took 15,5 hours on PC Linux machine. The computations with $M = 128$ took only 1,67 hours, but, of course, the precision is lower. It is important to note, see also the Table 2, that there are practically no differences in numerical solutions for $M = 128$ and $M = 384$ (so the picture was omitted for $M = 384$), but the computations for $M = 384$ took 2,5 hours.

The results of this example confirm our expectations. The FB-MOC with no CFL condition on the choice of time step is suitable for this type of coupled transport problems. There is only slight difference between numerical results for Courant number 9 and 3, but computations with Courant number 3 required twice longer computation time. Nevertheless, with smaller time steps (i.e. with smaller Courant number), the precision of numeri-

cal results will improve, and for Courant number bellow 1 the FB-MOC coincide with high-resolution finite volume methods.

Example 9.2. Finally, we briefly describes "typical" (two-dimensional) application of the software package R^3T (Retardation, Reaction, Radionuclides and Transport). At the top of Figure 4, the full picture of domain that is approximately 6 kilometres long and 150 m high, is plotted together with coarse computational grid. The zoomed pictures bellow show twice locally refined grid (the final grid was refined analogously 5 times) and some stationary velocity field that was obtained using the package D^3F [7].

The last three zoomed pictures at the bottom show numerical solution corresponding to concentrations of Americium, Neptunium and Uranium at some fixed time, where the contour lines represent 1% to 10% of the maximum value at this time point. Initially, there was no concentration in domain, and the time evolution of concentrations is caused by small time dependent source inside of the domain. All parameters in (1) are nonzero.

The porosity of the medium in the middle of domain is $\phi = 0.2$. The transport of Americium 241 (top picture) has the largest retardation factor $R^{Am} = 1001$, and it is spread only slightly outside of the source position. The middle picture shows the concentration of Neptunium 237 with $R^{Np} = 11$, and the last picture shows the concentration of Uranium 233 with $R^U = 8$.

The numerical solution was obtained with FB-MOC for Courant number equals approximately 9. We do not attempt to present here any rigourous analysis of this example, and more comprehensive description will be published elsewhere. This example is only small subproblem of origin problem with 26 components, and analogous problem is solved for three-dimensional domain.

10 Conclusions

The Flux-Based Methods Of Characteristics (FB-MOC) offer several advantages when compared with other Eulerian-Lagrangian methods. First of all, the FB-MOC are based on "flux-based" discretization schemes like Finite Volume Methods (FVM), and, consequently, they can share their popular properties - the discrete local and global mass conservation, straightforward treatment of general boundary conditions, and reduced numerical dispersion using high-resolution schemes. Moreover, they are formally not restricted by CFL condition on the choice of time steps, and they are free of unphysical oscillations for numerical solutions.

The most important advantages of FB-MOC is the possibility to couple numerical treatment of advection equations with other numerical (or exact) methods using "local form" of operator splitting methods. In such a way, large splitting errors, related to standard form of operator splitting methods, can be avoided.

The FB-MOC can be easily extended for advection problems with non-divergence free velocity field, i.e. for flows induced by sources and sinks, see [9]. Furthermore, an extension for nonlinear form of retardation factors $R = R(c)$, at least in one-dimensional case, is possible [17].

The simplest variants of FB-MOC without CFL restriction, as described here or in [8], exhibit expected numerical convergence rates approaching 1. Nevertheless, opposite to [8], the variant of FB-MOC described here that is based on high-resolution discretization methods, will improve with smaller time steps.

Finally, let us note that another perspective approach for further improvements of FB-MOC is the tracking of integration points instead of fractions of mass. Such approach, together with unlumped version of mass matrix [23], was successful in implementations of ELLAM [25], where grid effects and loss of peak concentrations could be reduced.

References

1. P. Bastian, K. Birken, K. Eckstein, K. Johannsen, S. Lang, N. Neuss, and H. Rentz-Reichert. UG - a flexible software toolbox for solving partial differential equations. *Computing and Visualization in Science*, 1(1):27–40, 1997.
2. P. Bastian and S. Lang. Couplex benchmark computations with UG. Technical Report 2002–31, IWR, Universität Heidelberg, 2002.
3. P. Binning and M.A. Celia. A finite volume Eulerian-Lagrangian localized adjoint method for solution of the contaminant transport equations in two-dimensional multiphase flow systems. *Water Resources Research*, 32(1):103–114, 1996.
4. Z. Cai, J. Mandel, and S. Mc Cormick. The finite volume element method for diffusion equations on general triangulations. *SIAM J. Numer. Anal.*, 28(2):392–402, 1991.
5. T. Prabhakar Clement. Generalized solution to multi-species transport equations coupled with a first-order reaction network. *Water Resources Research*, 37(1):157–163, January 2001.
6. P. Frolkovič. Maximum principle and local mass balance for numerical solutions of transport equation coupled with variable density flow. *Acta Mathematica Universitatis Comenianae*, 67(1):137–157, 1998.
7. P. Frolkovič. Discretization. In E. Fein, editor, *D^3F - ein Programmpaket zur Modellierung von Dichteströmungen*, Braunschweig, 1999. GRS-139, ISBN 3-923875-97-5, (see also http://www.iwr.uni-heidelelberg.de/∼Peter.Frolkovic).
8. P. Frolkovič. Flux-based method of characteristics for contaminant transport in flowing groundwater. *Computing and Visualization in Science*, 5(2):73–83, 2002.
9. P. Frolkovič. Flux-based methods of characteristics for transport problems in groundwater flow induced by sources and sinks. In S.M. Hassanizadeh, R.J. Schotting, W.G. Gray, and G.F. Pinder, editors, *Computational Methods in Water Resources 2*, pages 979–986. Elsevier, 2002.
10. P. Frolkovič and J. Geiser. Numerical simulations of radionuclides transport in double porosity media with sorption. In A. Handlovičova et al., editor, *Algoritmy 2000*, pages 28–36. Slovak University of Technology, Bratislava, 2000.

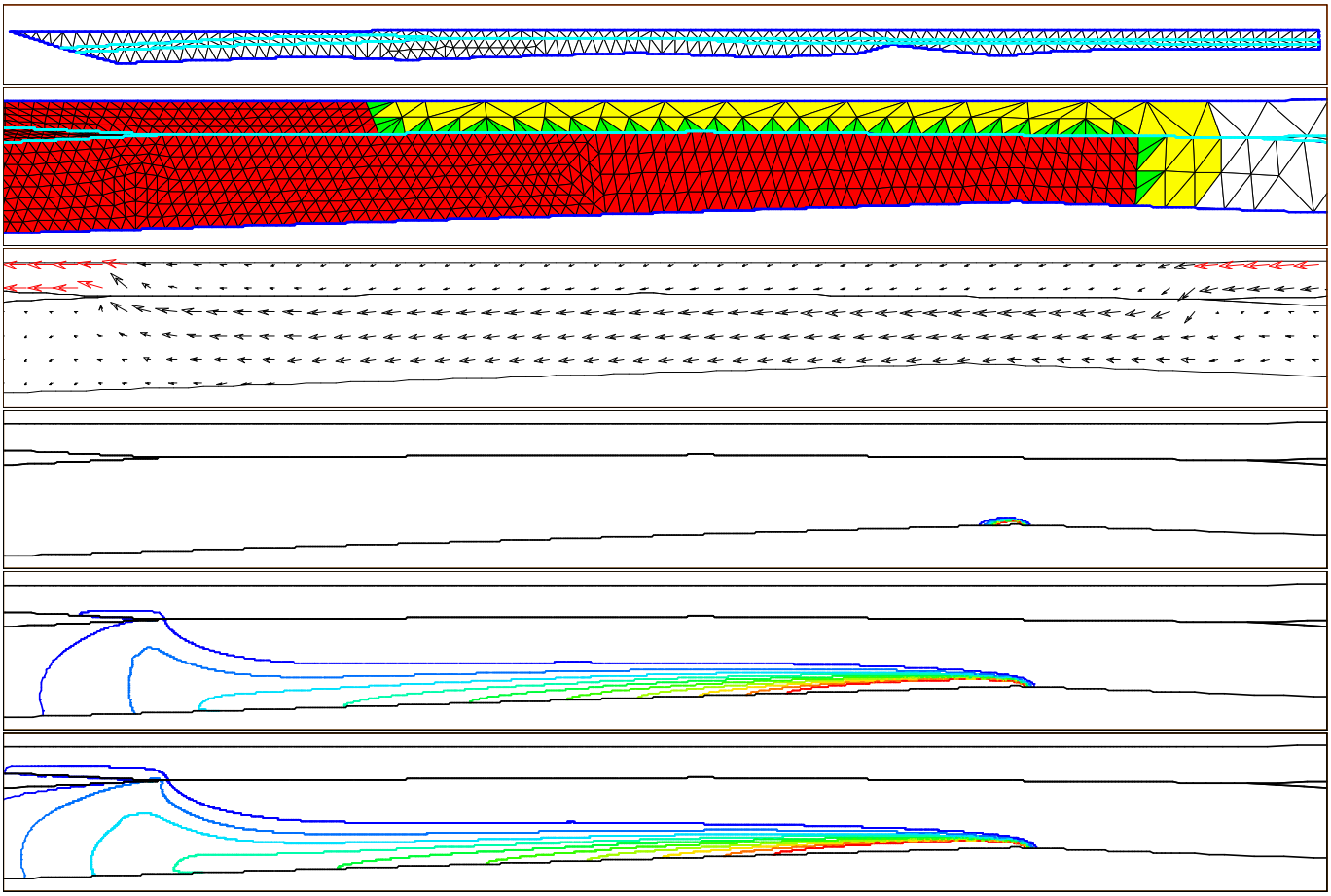

Fig. 4. From top to bottom - full picture of domain with coarse grid and zoomed pictures of twice locally refined grid, a velocity field and 3 components of numerical solution.

11. P. Frolkovič and J. Geiser. Discretization methods with discrete minimum and maximum property for convection dominated transport in porous media. In I. Dimov et al., editor, *Numerical Methods and Applications, Lecture Notes in Computer Science 2542*, pages 445–453. Springer-Verlag, Berlin Heidelberg, 2003.
12. P. Frolkovič and K. Mikula. Flux-based level set method, in preparation.
13. R.W. Healy and T.F. Russel. A finite-volume Eulerian-Lagrangian localized adjoint method for solution of the advection-dispersion equation. *Water Resources Research*, 29(7):2399–2413, 1993.
14. R.W. Healy and T.F. Russell. Solution of the advection-dispersion equation in two dimensions by a finite-volume Eulerian-Lagrangian localized adjoint method. *Advances in Water Resources*, 21(1):11–26, 1998.
15. T. Ikeda. *Maximum principle in finite element models for convection-diffusion phenomena.* North-Holland, Amsterdam, New York, Oxford, 1983.
16. K. Johannsen. Aligned 3d-finite-volumes for convection-diffusion-problems. In Vilsmeier R. Benkhaldoun F, editor, *Finite Volumes for Complex Applications*, pages 291–300. Hermes, Paris, 1996.
17. J. Kačur and P. Frolkovič. Semi-analytical solutions for contaminant transport with nonlinear sorption in 1D. Preprint 24, Interdisziplinäres Zentrum für Wissenschaftliches Rechnen, Oktober 2002.
18. Randall J. LeVeque. *Finite Volume Methods for Hyperbolic Problems.* Cambridge Texts in Applied Mathematics. Cambridge University Press, 2002.
19. B. Malengier. Dimensional splitting techniques for the flux based method of characteristics, in preparation.
20. M. Ohlberger. Higher order finite volume methods on selfadaptive grids for convection dominated reactive transport problems in porous media. Preprint 02-25, Mathematische Fakultät Freiburg, 2002.
21. S. V. Patankar. *Numerical heat transfer and fluid flow.* Hemisphere Publishing Corporation, 1980.
22. P.J. Roache. A flux-based modified method of characteristics. *Int. J. Numer. Methods Fluids*, 12:1259–1275, 1992.
23. T. Russell. Numerical dispersion in Eulerian-Lagrangian methods. In S.M. Hassanizadeh, R.J. Schotting, W.G. Gray, and G.F. Pinder, editors, *Computational Methods in Water Resources 2*, pages 963–970. Elsevier, 2002.
24. T. Russell. Private communication. November 2002.
25. T. F. Russell and M. A. Celia. An overview of research on Eulerian-Lagrangian localized adjoint methods (ELLAM). *Advances in Water Resources*, 25:1215–1231, 2002.
26. Th. Sonar. On the design of an upwind scheme for compressible flow on general triangulations. *Numerical Algorithms*, (4):135–149, 1993.